



 Cite this: *RSC Adv.*, 2024, 14, 29254

# Development of an electrochemical sensor modified with gold nanoparticles for detecting fumonisin B1 in packaged foods

 Liyuan Zhao, Longzhu Zhou, Dieudonné M. Dansou, Chaohua Tang, Junmin Zhang, Yuchang Qin\* and Yanan Yu \*

Fumonisin B1 (FB1) is naturally present in the environment and can easily contaminate packaged foods during processing, storage and transportation, thus posing a threat to human health. We have developed an enzyme-free FB1 detector for the detection of packaged foods, which provides rapid and sensitive detection of FB1 in food. Gold nanoparticles (AuNPs; 5–10 nm) were uniformly dispersed on screen-printed electrodes, which acted as an excellent catalytic oxidizer. The surface structure of the modified electrode was characterized using scanning electron microscope and X-ray photoelectron spectroscopy. Differential pulse voltammetry demonstrated a good linear electrochemical response towards FB1 at concentrations ranging from 1 ng L<sup>-1</sup> to 1 mg L<sup>-1</sup> with a detection limit of 0.08 ng L<sup>-1</sup>. We employed the AuNPs-SPE sensor to detect FB1-spiked packaged meat products achieving recovery rates ranging from 89.7% to 113.3%.

 Received 30th June 2024  
 Accepted 1st September 2024

DOI: 10.1039/d4ra04753b

[rsc.li/rsc-advances](https://rsc.li/rsc-advances)

## Introduction

According to the Food and Agriculture Organization (FAO), 25% of the world's food crops are affected by mycotoxin-producing fungi. In response to this threat, global efforts are underway to develop relevant standards.<sup>1</sup> China has not yet established a maximum limit standard for fumonisins in foods, and there is no unified international standard for the maximum limit of fumonisins in foods. However, the Joint Expert Committee of the FAO and the World Health Organization (WHO) on Food Additives has set the daily maximum tolerable intake of total FB1 at 2 µg per kg per day.<sup>2</sup> The European Union (EU) has established a maximum limit of 200 µg kg<sup>-1</sup> for fumonisins in corn products for infants and young children, as stated in the food safety standards for fumonisin.<sup>3</sup>

With the continuous improvement of people's quality of life, packaged meat and meat products have become an integral part of diets. However, contamination of packaged meat products with mycotoxins can originate from various sources and at all stages of the process, including harvesting, storage, transportation, and packaging, thereby attracting increasing attention.<sup>4,5</sup> Several studies have demonstrated that mycotoxin levels in meat and meat products pose a threat to human health. Therefore, to ensure the quality and safety of meat, it is essential to develop a sensitive measurement method for detecting meat FB1.<sup>6–8</sup>

Several methods have been developed to detect the FB1 content in foods. Among them, high-performance liquid chromatography, mass spectrometry, and thin layer chromatography are the most common. However, these methods often involve complex, time consuming, and expensive sample pre-treatment steps.<sup>9</sup> Sensors have emerged as a promising alternative for FB1 detection. While biosensors are susceptible to external environmental interference and immune crossover, compromising detection stability,<sup>10</sup> electrochemical sensors offer a simple, portable, and sensitive detection tool that can quickly detect FB1 in foods at a low cost.

Screen-printed electrodes (SPEs) are commonly used in electrochemical sensors constructed on plastic or ceramic substrates through thick film deposition technology, allowing for simple, inexpensive, and fast on-site analyses with high reproducibility, sensitivity, and accuracy.<sup>11</sup> Precious metals and transition metals, such as gold (Au), silver, platinum, and titanium, are often employed in electrode construction to enhance the electrical signal conductivity of SPEs. Precious metals offer stable chemical properties, adequate biocompatibility, and excellent conductivity. Gold nanoparticles (AuNPs) are particularly noteworthy in sensing applications due to their unique optical and electronic properties.<sup>12,13</sup> The small size of gold nanoparticles exposes more surface groups, contributing to their excellent catalytic properties.<sup>14</sup> Ion implantation is the process of ionizing atoms of a specified element, which, under the action of an electric field, achieve a high velocity and deposited onto the surface of a solid material. Ions can be uniformly embedded into the substrate surface to form stable metal particles at the nanometer level.<sup>15</sup>

State Key Laboratory of Animal Nutrition and Feeding, Institute of Animal Science, Chinese Academy of Agricultural Sciences, Beijing, 100193, China



Ion implantation is an effective surface modification technology for materials, where a small number of ions can change the conductivity of the main material by several orders of magnitude. This technology does not require any binders or chemicals, making it environmentally friendly and easy to perform.<sup>16,17</sup>

In this study, we used ion implantation to modify an SPE with AuNPs, thereby developing an AuNPs-SPE. Subsequently, we used this sensor to detect FB1 in food by differential pulse voltammetry (DPV).

## Materials and methods

### Chemicals and reagents

We obtained FB1 (99% purity) from Shanghai Yuanye Bio-Technology Co Ltd (Shanghai, China) and SPEs from Metrohm-Dropsens (Shanghai, China). We prepared 0.1 M phosphate buffer saline (PBS) of different pH values by mixing 0.1 M  $\text{NaH}_2\text{PO}_4$  and  $\text{Na}_2\text{HPO}_4$ . A standard FB1 stock solution ( $100 \text{ mg mL}^{-1}$ ) was prepared by dissolving FB1 in water. Possible interfering compounds, such as glutamic acid, cystine, tartaric acid, fructose, sucrose, and vitamin B2, were prepared at concentrations of  $10 \text{ g L}^{-1}$  in ultrapure water. Glutamic acid, cystine, and vitamin B2 were first dissolved in an alkaline solution. Before use, SPE was cleaned with ultrapure water and dried with  $\text{N}_2$  gas to prevent electrode oxidation. DPV and cyclic voltammetry were commonly used to characterize the electrochemical characteristics of SPEs. Comparatively, DPV is more sensitive than cyclic voltammetry; therefore, we used DPV to quantify FB1. The potential range was set from 0 to 0.8 V, and the scanning speed was  $100 \text{ mV S}^{-1}$ . All experiments were conducted at room temperature.

### Instruments

All electrochemical measurements were performed using a CHI660E electrochemical workstation (Chenhua Instrument Company, Shanghai, China) in a three-electrode system. The reference electrode and electric contacts were made of silver. The pH values of the buffer solutions were determined using a pH meter (Mettler Toledo Instrument Company, Shanghai, China). For the Au ion implantation process, the acceleration voltage was set at 10 keV, and the injection dose was  $1 \times 10^{17}$  ions  $\text{cm}^{-2}$ . The surface morphology was observed using scanning electron microscopy (SEM; SU8020 microscope, Hitachi, Japan). X-ray photoelectron spectroscopy (XPS) was performed using a Thermo Escalab 250 XI (Thermo Scientific, Britain, Europe) with an Al Ka X-ray source.

### Preparation of real samples

We purchased packaged pork and beef separately from the local market. The samples were ground and mixed with 10 mL of 0.1 M PBS, the sonicated for 30 min, and subsequently centrifuged for 10 min at  $25\,000\times g$ . Following the removal of meat fat, we diluted the supernatant  $20\times$  for electrochemical detection.

## Results

### Validation of electrode modification

**Surface characterization.** The surface characterization of the SPEs was studied by SEM and AFM (Fig. 1). The characteristics of the Bare SPE surface characteristics are shown in Fig. 1A, and the AuNPs-SPE surface in Fig. 1B. In the bare SPE, we observed spherical structures of varying sizes, with diameters ranging from 100 to 400 nm. Ion implantation transformed the surface structure of the electrodes, causing a larger and denser arrangement of carbon elements. Specifically, in the AuNPs-SPE, we observed spherical structures of around 5 to 10 nm, which were densely and evenly deposited on the surface. A plethora of studies have demonstrated that the size, the distinct shape, and the specific morphology of AuNPs exert a significant influence on the intrinsic performance of nanomaterials.<sup>18,19</sup> For instance, smaller-sized AuNPs tend to exhibit enhanced catalytic activity due to their higher surface-to-volume ratio. Meanwhile, differently shaped AuNPs, such as rods or stars, may possess unique optical properties. The AFM 2D and 3D surface morphology of bare SPE and AuNPs-SPE as shown in Fig. 1E–H reveal that after the implantation of Au nano ions, the

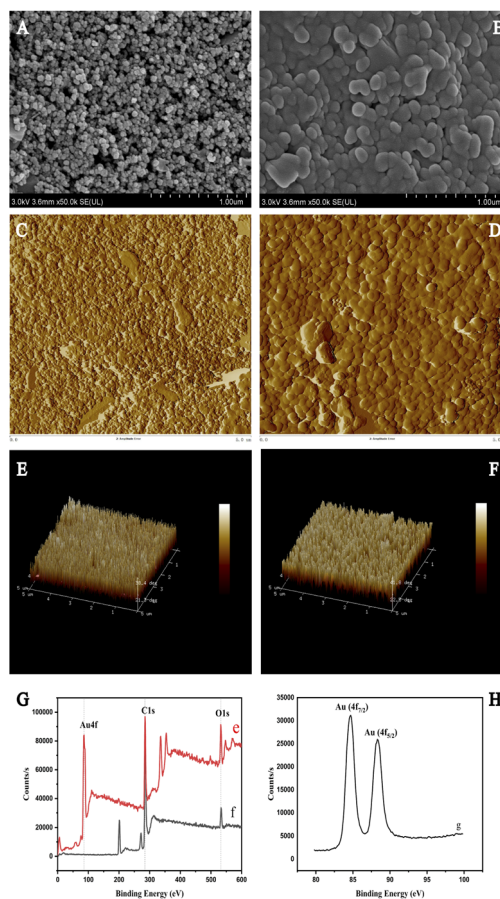


Fig. 1 SEM images of bare SPE ( $\times 50 \text{ k}$ ; A) and of AuNPs-SPE ( $\times 50 \text{ k}$ ; B). The AFM 2D and 3D surface morphology of bare SPE (C and E) and of AuNPs-SPE (D and F). XPS images of the AuNPs-SPE sensor (G), Au 4f (H); AuNPs-SPE (E), bare SPE (F), AuNPs-SPE (G).



arrangement of carbon elements becomes larger and denser, which share similarities with the SEM results.

**XPS.** We employed XPS to evaluate the state of both the bare SPE and AuNPs-SPE, focusing on the surface elemental composition and chemical states.<sup>20</sup> As depicted in Fig. 1E, no Au peak was observed within the same energy range, for the bare SPE. However, following ion implantation, there was an evident Au peak in the AuNPs-SPE, and Au 4f could be clearly observed. In Fig. 1F, Au (4f<sub>7/2</sub>) at 84.67 eV and Au (4f<sub>5/2</sub>) at 88.29 eV were visible and confirm successful AuNPs implantation on the SPE surface.<sup>21–23</sup>

**Optimization of experimental conditions.** To obtain more sensitive detection outcomes, we optimized the buffer pH for electrochemical detection. pH plays a crucial role in influencing various aspects of proton-coupled electron transfer reactions in electrochemical systems. The influence of pH on the electrochemical behavior of the AuNPs-SPE was investigated by cyclic voltammetry within the pH range from 4 to 8. The cathodic peak current increases with increasing pH values, reaching its maximum at pH 7.4, as depicted Fig. 2. Beyond pH 7.4, the cathodic peak current began to decrease. Therefore, pH 7.4 was determined as the optimal condition for electrochemical detection of the electrode, which is consistent with previous studies.<sup>24</sup> Eventually, subsequent experiments were carried out with PBS at pH 7.4.

### Detection ability of the sensor

**Surface characterizations.** Fig. 3 shows the CV response (Fig. 3A) and DPV response (Fig. 3B) of the bare SPE and AuNPs-SPE in 0.1 M PBS, respectively. Compared to the bare SPE, the AuNPs-SPE had a higher peak current. DPV measurements were conducted on both the bare SPE and AuNPs-SPE in PBS with and without 1 mg L<sup>-1</sup> FB1. Interestingly, the DPV results of the bare SPE with and without 1 mg L<sup>-1</sup> FB1 were nearly identical. In contrast, the AuNPs-SPE displayed enhanced electronic conductivity with an obvious electrochemical response in the presence of 1 mg L<sup>-1</sup> FB1. The CV response (Fig. 3A) and DPV response (Fig. 3B) of both the bare SPE and the AuNPs-SPE outcomes clearly indicate that the redox peak that was

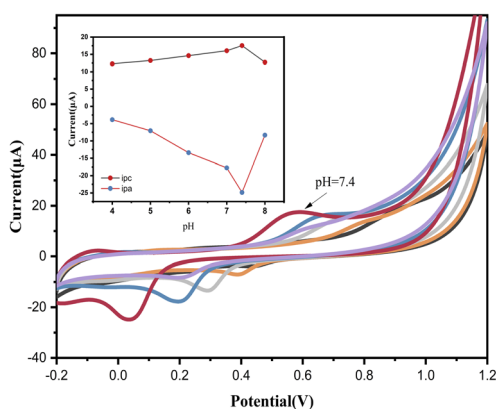


Fig. 2 Cyclic voltammograms (CVs) of 0.1 M PBS of different pH values (4, 5, 6, 7, 7.4, 8). Inset: the influence of pH on the current.

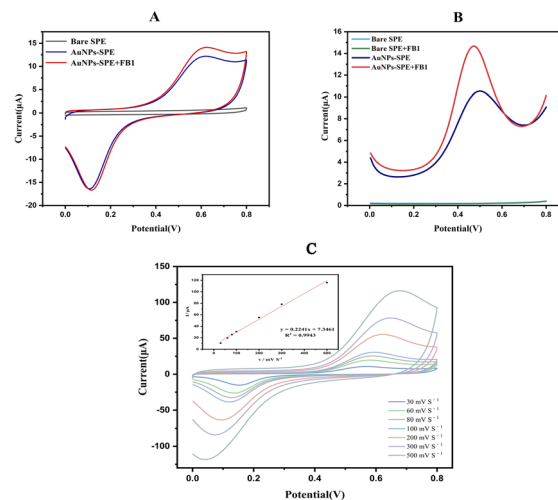
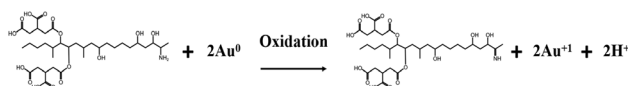


Fig. 3 (A) CVs of FB1 (0.1 mg L<sup>-1</sup>) in 0.1 M PBS (pH = 7.4) of the bare SPE and AuNPs-SPE. (B) DPVs of FB1 (0.1 mg L<sup>-1</sup>) in 0.1 M PBS (pH = 7.4) of the bare SPE and AuNPs-SPE. The blue line coincides with the green line. (C) The CV of 10 mL PBS in 0.1 M FB1 on the AuNPs-SPE.

observed in the case of the AuNPs-SPE was significantly higher than that of the bare SPE. This observation firmly confirms that the AuNPs exerted a pronounced catalytic effect on the redox reaction of FB1. The process of ion implantation involving AuNPs brought about an improvement in the electrochemical detection capability. During the process of electrochemical detection of FB1 employing the AuNPs-SPE, the remarkable increase in oxidation current that was observed can be primarily attributed to the specific reaction between Au<sup>0</sup> and FB1 (Scheme 1).

**Kinetics studies.** The kinetic parameters of the AuNPs-SPE in FB1 standard solution were determined using cyclic voltammetry detection at various scanning speeds (Fig. 3C). As the scanning rate increased, the oxidation peak potential shifted positively, while the reduction peak potential shifted negatively. Therefore, the peak current values for oxidation and reduction are positively correlated with the scanning rate. The derived equations and correlation coefficient were  $I_{pa} = 0.2241v + 7.3461$  and  $R^2 = 0.9943$ , respectively, indicating that the reaction between the electrode and FB1 is a typical adsorption-controlled process.<sup>25</sup>

**Determination of FB1.** DPV effectively eliminates background current effect and offers higher sensitivity, making it suitable for quantitative research. The AuNPs-SPE exhibited distinct electrochemical responses at different concentrations of FB1 (Fig. 4). The peak current obtained by DPV detection increased with increasing FB1 concentration ( $I_p = 0.5778 \lg C + 12.8486$ ,  $R^2 = 0.9907$ , where  $C$  is the concentration of FB1). Electron transfer is facilitated in the presence of FB1.<sup>26</sup> The limit



Scheme 1 The electrooxidation mechanism of FB1.



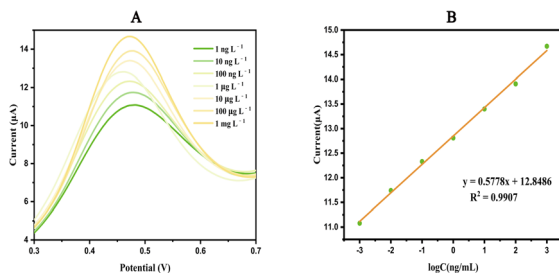


Fig. 4 (A) DPVs of FB1 with different concentrations of the AuNPs-SPE. FB1 concentrations ranged from  $1 \text{ ng L}^{-1}$  to  $1 \text{ mg L}^{-1}$ . The concentration of the next one is 10 times that of the previous one. (B) Linear relationship between current intensity and the concentration of FB1.

of detection (LOD) of FB1 was determined to be  $0.08 \text{ ng L}^{-1}$  based on the equation  $\text{LOD} = 3\text{Sd}/b$ , where Sd is the standard deviation of the electrochemical response of the blank solution for 30 cycles, and Fig. 4B is the slope of the calibration curve.

**Selectivity studies.** Common food constituents such as fructose, sucrose, glutamic acid, and cystine were evaluated for potential interference in FB1 detection using the AuNPs-SPE. The sensor was tested against  $1 \text{ mg L}^{-1}$  FB1 and concentrations of fructose, sucrose, glutamic acid, cystine, tartaric acid, and vitamin B2 at 50 times, as well as 100 times the concentration of anhydrous ethanol (Fig. 5). Only FB1 exhibited a significant electrochemical response, indicating that our developed sensor has a high anti-interference ability. AuNPs-SPE effectively avoids interference from similar substances, ensuring both the accuracy and reliability of the detection results related to FB1.

**Stability studies.** DPV was used to detect the peak current of four different AuNPs-SPEs at the same time (Fig. 6A). There was good consistency in electrochemical response between different electrodes ( $\text{RSD} = 3.8\%$ ). After 30 consecutive scans, the RSD was 1.6%, indicating that the electrode has good anti-fouling ability. This high consistency indicates that under the same experimental conditions, different AuNPs-SPEs electrodes display similar and stable electrochemical behaviors. This is of great significance for research and applications that require

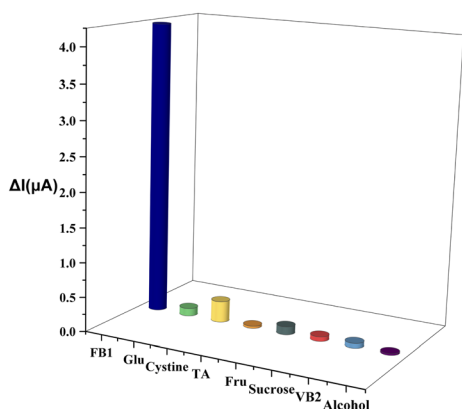


Fig. 5 Detection of multiple compounds by the AuNPs-SPE. The concentration of FB1 was  $1 \text{ mg mL}^{-1}$ .

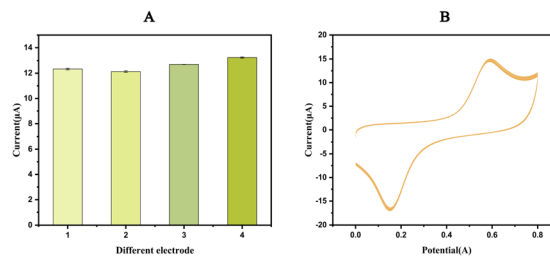


Fig. 6 (A) Bar plots of the cathodic peak current of four different AuNPs-SPEs. (B) Thirty CV results of the AuNPs-SPE in PBS.

reliable and repeatable measurement results. It reduces the errors and uncertainties that might be caused by individual differences among electrodes and provides a solid basis for further analysis and conclusions.

**Detection of real samples.** To assess the applicability of our electrochemical sensors to real packaged foods, we employed AuNPs-SPE to analyze packaged pork and beef spiked with FB1, simulating foods that may be contaminated during production, transportation, and packaging (Table 1). The FB1 recovery rates ranged between 89.7% and 113.3%. These results demonstrate that the AuNPs-SPE can be used to detect FB1 in meat with high accuracy and sensitivity.

The detection performance of the proposed sensor was compared with other existing methods for FB1 detection, and the results were summarized in Table 2. Our sensor demonstrates excellent sensitivity. Additionally, most of the aptasensor and fluorescence methods need to be combined with immunoassays, which increase the complexity of the operation. In contrast, the electrochemical sensor is simple to operate and does not require exquisite equipment, which can meet the need of easy and practical monitoring of FB1.

## Discussion

It is well known that FB1 is harmful to animal and human health, often causing imperceptible contamination of packaged foods at various stages of production and distribution. As a result, residues of FB1 in packaged foods should be strictly controlled. The presence of FB1 in packaged meat products can be easily overlooked. Therefore, the development of a simple methodology for the detection of FB1 is of great value in food toxin detection.

Many methods still suffer from low sensitivity, complexity of production, and are rarely considered for the detection of FB1 in

Table 1 Determination and recovery of FB1 in samples using the AuNPs-SPE ( $n = 3$ )

Samples	Spiked ( $\mu\text{g L}^{-1}$ )	Detected ( $\mu\text{g L}^{-1}$ )	Recovery%	RSD ( $n = 3$ )%
Pork	1	$1.13 \pm 0.03$	113.0	2.2
	5	$4.48 \pm 0.11$	89.7	2.4
	10	$10.08 \pm 0.20$	100.8	2.0
Beef	1	$1.13 \pm 0.05$	113.3	4.5
	5	$5.04 \pm 0.15$	100.8	2.9
	10	$11.96 \pm 0.04$	101.2	0.4



Table 2 A comparison of the analytical methods for the detection of FB1

Method	Samples	Linear range	LOD	Ref.
Fluorescence resonance energy transfer	Maize	0–3000 ng mL <sup>-1</sup>	14.42 ng mL <sup>-1</sup>	27
Electrochemical aptasensor	Maize	0.5–500 ng mL <sup>-1</sup>	0.14 ng mL <sup>-1</sup>	28
Colorimetric sensor	Cereal	3–200 ng mL <sup>-1</sup>	1.73 µg L <sup>-1</sup>	29
Paper-based electrochemical aptasensor	Wheat	50 fg mL <sup>-1</sup> –100 ng mL <sup>-1</sup>	—	30
ELISA	Garlic	0.25–0.50 mg L <sup>-1</sup>	0.25 mg L <sup>-1</sup>	31
This work	Pork Beef	1 ng L <sup>-1</sup> –1 mg L <sup>-1</sup>	0.08 ng L <sup>-1</sup>	—

packaged meat products. Traditional detection methods of FB1 include thin-layer chromatography, high-performance liquid chromatography, gas chromatography/mass spectrometry, and immunosorbent assays.<sup>32–34</sup> These methods have several limitations, such as complex pre-treatment and the use of toxic solvents.<sup>35</sup> In recent years, numerous new methods have emerged for detecting mycotoxins. However, few methods are available for detecting FB1 in foods, especially in meat. Electrochemical detection technology is a well-established technique for detection and analysis.

Our method offers high sensitivity and a low detection limit (LOD) which can be applied for a rapid detection of meat mycotoxins. AuNPs are commonly used as metal modification materials, which are easily synthesized, exhibit high reaction interface activity, reduce the energy barrier of electrochemical redox reactions, and demonstrate have adequate electrochemical performance.<sup>36</sup> We modified a certain size of AuNPs on the SPE surface by ion implantation and characterized the surface morphology and microstructure of bare and AuNPs-SPE by SEM and found that AuNPs were uniformly and densely distributed on the SPE surface.

The CV response (Fig. 3A) and DPV response (Fig. 3B) of the bare SPE and AuNPs-SPE results indicate that the redox peak observed with the AuNPs-SPE was notably higher than that of the bare SPE, confirming that the AuNPs exerted a catalytic effect on the redox reaction of FB1. Ion implantation with AuNPs improved the electrochemical detection capability and optimized the detection conditions to improve the binding of FB1. Consequently, AuNPs-SPE demonstrated highly sensitive FB1 detection capabilities and can be used as an effective tool for detecting FB1 in packaged foods.

## Conclusions

To conclude, AuNPs-SPEs do not require complex pre-processing steps. FB1 can be rapidly and sensitively quantified in packaged foods using DPV. AuNPs-SPEs has good stability, reproducibility, and specificity, with a detection limit of 0.08 ng L<sup>-1</sup> for FB1. SPE was modified by ion implantation, which improved the conductivity of the electrode and provided a novel method for the detection of mycotoxins in packaged foods.

## Data availability

Data will be made available on request.

## Author contributions

Liyuan Zhao: validation, software, formal analysis, methodology, writing – original draft. Longzhu Zhou: investigation, validation. Dieudonné M. Dansou: writing – review & editing, validation. Chaohua Tang: resources, writing – review & editing. Junmin Zhang: writing – review & editing, funding acquisition, supervision. Yuchang Qin: supervision, funding acquisition. Yanan Yu: conceptualization, supervision, methodology, funding acquisition.

## Conflicts of interest

The authors declare that they have no known competing financial interests or personal relationships that could have appeared to influence the work reported in this paper.

## Acknowledgements

This research was supported by the National Natural Science Foundation of China (32102590), Chongqing Rongchang Agriculture and Animal Husbandry High Tech Industry Research and Development Project (cstc2020ngzx0005) and the Chinese Academy of Agricultural Science and Technology Innovation Project (ASTIP-IAS-12).

## Notes and references

- 1 C. Levasseur-Garcia, *Toxins*, 2018, **10**, 8.
- 2 G. S. Shephard, H.-M. Burger, J. P. Rheeder, J. F. Alberts and W. C. A. Gelderblom, *Food Control*, 2019, **97**, 77–80.
- 3 L. Qu, L. Wang, H. Ji, Y. Fang, P. Lei, X. Zhang, L. Jin, D. Sun and H. Dong, *Toxins*, 2022, **14**, 182.
- 4 J. Pleadin, D. Kovačević and N. Perši, *Food Control*, 2015, **57**, 377–384.
- 5 S. M. Abd-Elghany and K. I. Sallam, *Food Chem.*, 2015, **179**, 253–256.
- 6 M. Sokolovic, M. Berendika, T. Amsel Zelenika, B. Simpraga and F. Krstulovic, *Toxins*, 2022, **14**, 444.
- 7 A. R. Alaboudi, T. M. Osaili and G. Otoum, *Food Control*, 2022, **132**, 108511.
- 8 C. Juan, S. Oueslati, J. Manes and H. Berrada, *J. Food Sci.*, 2019, **84**, 3885–3893.
- 9 X. Chen, H. Wu, X. Tang, Z. Zhang and P. Li, *Electroanalysis*, 2021, **35**, 210022.



- 10 Y. Xiang, M. B. Camarada, Y. Wen, H. Wu, J. Chen, M. Li and X. Liao, *Electrochim. Acta*, 2018, **282**, 490–498.
- 11 G. Paimard, E. Ghasali and M. Baeza, *Chemosensors*, 2023, **11**, 113.
- 12 L. Tu, *Gold Bull.*, 2022, **55**, 169–185.
- 13 Y. Zhong, P. Liao, J. Kang, Q. Liu, S. Wang, S. Li, X. Liu and G. Li, *J. Am. Chem. Soc.*, 2023, **145**, 4659–4666.
- 14 Z. Wang, Y. Shao, Z. Zhu, J. Wang, X. Gao, J. Xie, Y. Wang, Q. Wu, Y. Shen and Y. Ding, *Coord. Chem. Rev.*, 2023, **495**, 215369.
- 15 D. Gupta and R. Kumar, *Mater. Sci. Semicond. Process.*, 2023, **158**, 107326.
- 16 S. D. Pravesh, D. Singh and M. Singh, *Pramana*, 2023, **97**, 58.
- 17 A. K. Manna, A. Kanjilal, D. Kanjilal and S. Varma, *Nucl. Instrum. Methods Phys. Res., Sect. B*, 2020, **474**, 68–73.
- 18 R. El-Sayed, F. Ye, H. Asem, R. Ashour, W. Zheng, M. Muhammed and M. Hassan, *Biochem. Biophys. Res. Commun.*, 2017, **491**, 15–18.
- 19 J. Wu, X. Wang, Q. Wang, Z. Lou, S. Li, Y. Zhu, L. Qin and H. Wei, *Chem. Soc. Rev.*, 2019, **48**, 1004–1076.
- 20 M. Keerthi, A. Kumar Panda, Y. H. Wang, X. Liu, J. H. He and R. J. Chung, *Food Chem.*, 2022, **378**, 132083.
- 21 F. Y. Kong, R. F. Li, L. Yao, Z. X. Wang, H. Y. Li, W. J. Wang and W. Wang, *Nanotechnology*, 2019, **30**, 285502.
- 22 Y. Luo, F.-Y. Kong, C. Li, J.-J. Shi, W.-X. Lv and W. Wang, *Sens. Actuators, B*, 2016, **234**, 625–632.
- 23 R. Devi, S. Gogoi, S. Barua, H. Sankar Dutta, M. Bordoloi and R. Khan, *Food Chem.*, 2019, **276**, 350–357.
- 24 A. R. Cardoso, F. T. C. Moreira, R. Fernandes and M. G. F. Sales, *Biosens. Bioelectron.*, 2016, **80**, 621–630.
- 25 K. Li, J. Cui, Q. Yang, S. Wang, R. Luo, A. Rodas-Gonzalez, P. Wei and L. Liu, *Food Chem.*, 2023, **405**, 134791.
- 26 Z. Han, Z. Tang, K. Jiang, Q. Huang, J. Meng, D. Nie and Z. Zhao, *Biosens. Bioelectron.*, 2020, **150**, 111894.
- 27 X. Zhao, J. Gao, Y. Song, J. Zhang and Q. Han, *Sensors*, 2022, **22**, 8598.
- 28 B. Naghshbandi, M. Adabi, K. Pooshang Bagheri and H. Tavakolipour, *J. Nanobiotechnol.*, 2023, **20**, 534.
- 29 X. Niu, H. He, H. Ran, Z. Wu, Y. Tang and Y. Wu, *Food Chem.*, 2023, **429**, 136903.
- 30 X. Zhang, Z. Li, L. Hong, X. Wang and J. Cao, *J. Agric. Food Chem.*, 2023, **71**, 19121–19128.
- 31 S. Tonti, M. Mandrioli, P. Nipoti, A. Pisi, T. G. Toschi and A. Prodi, *J. Agric. Food Chem.*, 2017, **65**, 7000–7005.
- 32 Q. Zhou, F. Li, L. Chen and D. Jiang, *J. Food Sci.*, 2016, **81**, T2886–T2890.
- 33 J. He, B. Zhang, H. Zhang, L. L. Hao, T. Z. Ma, J. Wang and S. Y. Han, *J. Food Sci.*, 2019, **84**, 2688–2697.
- 34 M. Zhang, X. Guo and J. Wang, *Biosens. Bioelectron.*, 2023, **224**, 115077.
- 35 S. Z. Iqbal, S. Nisar, M. R. Asi and S. Jinap, *Food Control*, 2014, **43**, 98–103.
- 36 Y. Ju, H. Zhang, J. Yu, S. Tong, N. Tian, Z. Wang, X. Wang, X. Su, X. Chu, J. Lin, Y. Ding, G. Li, F. Sheng and Y. Hou, *ACS Nano*, 2017, **11**, 9239–9248.

